Computers in Biology and Medicine 139 (2021) 104950

Contents lists available at ScienceDirect

Computers in Biology and Medicine

journal homepage: www.elsevier.com/locate/compbiomed

Predicting fluid-response, the heart of hemodynamic management: A model-based solution

Rachel Smith [a,*], Christopher G. Pretty [a], Geoffrey M. Shaw [b], Thomas Desaive [c], J. Geoffrey Chase [a]

[a] Department of Mechanical Engineering, University of Canterbury, New Zealand
[b] Christchurch Hospital Intensive Care Unit, New Zealand
[c] GIGA - In Silico Medicine, University of Liège, Liège, Belgium

ARTICLE INFO

Keywords:
Hemodynamic monitoring
Intensive care unit
Fluid resuscitation
Fluid responsiveness
Mathematical modelling

ABSTRACT

Background: Intravenous fluid infusions are an important therapy for patients with circulatory shock. However, it is challenging to predict how patients' cardiac stroke volume (SV) will respond, and thus identify how much fluids should be delivered, if any. Model-predicted SV time-profiles of response to fluid infusions could potentially be used to guide fluid therapy.

Method: A clinically applicable model-based method predicts SV changes in response to fluid-infusions for a pig trial (N = 6). Validation/calibration SV, SV_{mea}, is from an aortic flow probe. Model parameters are identified in 3 ways: fitting to SV_{mea} from the entire infusion, SV_{fl}^{fit}, from the first 200 ml, SV_{fl}^{200}, or from the first 100 ml, SV_{fl}^{100}. RMSE compares error of model-based SV time-profiles for each parameter identification method, and polar plot analysis assesses trending ability. Receiver-operating characteristic (ROC) analysis evaluates ability of model-predicted SVs, SV_{fl}^{200} and SV_{fl}^{100}, to distinguish non-responsive and responsive infusions, using area-under the curve (AUC), and balanced accuracy as a measure of performance.

Results: RMSE for SV_{fl}^{Fit}, SV_{fl}^{200}, and SV_{fl}^{100} was 1.8, 3.2, and 6.5 ml, respectively, and polar plot angular limit of agreement from was 11.6, 28.0, and 68.8°, respectively. For predicting responsive and non-responsive interventions SV_{fl}^{200}, and SV_{fl}^{100} had ROC AUC of 0.64 and 0.69, respectively, and balanced accuracy was 0.75 in both cases.

Conclusions: The model-predicted SV time-profiles matched measured SV trends well for SV_{fl}^{Fit}, SV_{fl}^{200}, but not SV_{fl}^{100}. Thus, the model can fit the observed SV dynamics, and can deliver good SV prediction given a sufficient parameter identification period. This trial is limited by small numbers and provides proof-of-method, with further experimental and clinical investigation needed. Potentially, this method could deliver model-predicted SV time-profiles to guide fluid therapy decisions, or as part of a closed-loop fluid control system.

1. Introduction

Intravenous fluid infusions are an important therapy for patients with circulatory shock [1]. However, only half of hemodynamically unstable patients are fluid responsive [2] and unneeded fluid therapy leads to fluid overload, and increasing ICU stay and mortality [3–5]. Thus, it is crucial to identify whether patients are fluid responsive, defined as an increase in cardiac output (CO) or stroke volume (SV) $\geq$ 10 – 15% after a fluid challenge of 250–500 ml [2,6].

Numerous metrics for assessing fluid responsiveness exist, as discussed in Refs. [1,7]. Dynamic measurements are more useful than static metrics, which do not reliably indicate fluid responsiveness [1,7]. Consensus statements say fluid therapy should be targeted using flow based metrics, SV and CO, rather than pressures [8]. Additionally, echocardiography is a useful, but intermittent tool to assess cardiac function, providing information about preload, afterload and contractility [1]. However, none of the metrics currently available can accurately predict fluid response time-profiles, or fluid responsiveness, so successful fluid therapy remains an uncertain proposition [9].

Simple lumped-parameter models in Refs. [10,11] relate fluid

* Corresponding author.
E-mail address: rachel.smith@pg.canterbury.ac.nz (R. Smith).

https://doi.org/10.1016/j.compbiomed.2021.104950
Received 30 August 2021; Received in revised form 28 September 2021; Accepted 13 October 2021
Available online 15 October 2021

infusion time-profiles to blood volume and SV response, respectively. The 3-parameter model in Ref. [10] describes blood volume response to fluids as a proportional controller, and accurately fits observed dynamics. This model is extended by Ref. [11] for which blood volume response to fluids and hemorrhage is modelled as a proportional-integral (PI) controller. SV, CO, and blood pressure changes are then estimated using two additional models. Overall, 8 parameters are required to provide an SV output from an input fluid time-profile and an input heart rate time-profile, and the model fits experimental data well. This model-based approach of [10,11] can potentially allow prediction of fluid-responsiveness and closed-loop fluid control, a holy grail for critical-care [11–13]. However, the model from Ref. [11] requires 8 parameters to provide an SV output, and the model's ability to predict fluid responsiveness has not been directly assessed.

This study presents a model-based method to predict SV changes in response to a series of fluid-infusions for a pig trial. The model is similar to Refs. [10,11], but with reduced complexity, making it easy to interpret, and requiring identification of only 4 parameters. Model parameters are identified from a measured SV input from either the entire fluid infusion, or just the first 100 ml or 200 ml, and in each case the model performance is compared. The outcome is a simple, clinically-applicable model which can deliver predicted SV response time-profiles to an input fluid infusion time-profile.

2. Materials and methods

2.1. Porcine trials and measurements

Pig experiments were conducted at the Centre Hospitalier Universitaire de Liège, Belgium and approved by the Ethics Committee of the University of Liège Medical Faculty, permit number 14–1726.

A total of 6 Pure Piétrain pigs were used, weighing 18.5 kg–29.0 kg. Diazepam (1 mg kg^{-1}) and tiletamine-zolazepam (0.1 ml kg^{-1}, containing 25 mg ml^{-1} tiletamine and 25 mg ml^{-1} zolazepam) were used for initial sedation and anesthesia. A continuous infusion of sufentanil (0.1 ml kg^{-1} h^{-1} at 0.005 mg ml^{-1}), thiobarbital (0.1 ml kg^{-1} h^{-1}) and cisatracurium besylate (1 ml kg^{-1} h^{-1} at 2 mg ml^{-1}) were used to maintain sedation and anesthesia, delivered via superior vena cava catheter. Pigs were mechanically ventilated via tracheostomy with baseline positive end-expiratory pressure (PEEP) of 5 cmH_2O and tidal volume of 10 ml kg^{-1} delivered by a GE Engstrom Care Station mechanical ventilator (GE 92 Healthcare, Waukesha, WI, USA).

Blood pressure was measured in the proximal aorta (P_{ao}), femoral artery (P_{fem}), and vena cava (P_{cv}) using high fidelity pressure catheters (Transonic, Ithaca, NY, USA). Left ventricle pressures and volumes (V_{LV}) were measured using 7F micromanometer-tipped admittance catheters (Transonic, Ithaca, NY, USA). Aortic flow (Q_{ao}) was measured from an ultrasonic aortic flow probe positioned around the proximal aorta near the aortic valve (Transonic, Ithaca, NY, USA). Once the probe was located, the thorax was held closed using clamps. All data was recorded at a sampling rate of 250 Hz as a single Notocord data file (Instem, Croissy-sur-Seine, France). Signals were filtered with a 5th order Butterworth low-pass filter, with a cut-off frequency of 20 Hz (P_{fem}, P_{ao}, P_{cv}) and 10 Hz for noisier signals (V_{LV}, Q_{ao}).

Pigs were given 3 fluid infusions of 500 ml of saline solution over 30 min to increase circulatory volume and ventricular preload. After each 100 ml of fluid was delivered, there was an end expiratory pause, in which the ventilator is paused at end-expiration for 20 s. The effect of this pause is to increase cardiac preload, and thus SV [14]. Between the first and second fluid infusion, pigs were given an infusion of endotoxin (E. Coli lipopolysaccharide at 0.5 mg kg^{-1} over 30 min) to produce a septic shock like response [15]. Pigs 1, 3, and 6 died during the endotoxin infusion. Fig. 1 shows the fluid infusions delivered for each pig.

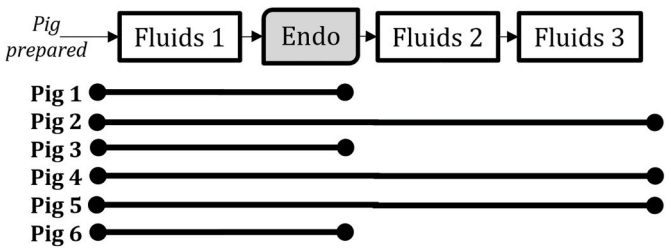

Fig. 1. Time-schedule of fluid infusions (Fluids) and endotoxin infusion (Endo) for each pig.

2.2. Measurement of SV

Measured SV (SV_{mea}) obtained from integrating Q_{ao} over one beat is used for validation and calibration. Beats are separated using the foot of Q_{ao}, identified using a shear-transform algorithm [16]. Flow probes are quoted as having precision of ±2% [17]. Pig 1 flow probe was faulty, delivering non-physiological waveforms, and for this pig SV_{mea} is obtained from admittance catheter V_{lv} as the difference between maximum and minimum V_{lv} over one beat. Admittance catheter SV has Bland-Altman mean bias [limits of agreement (±1.96 standard dev.)] of 6% [± 29%] using 3D-echocardiography as a reference method [18]. Clinically, SV_{mea} for calibration could be obtained non-invasively using echocardiography.

2.3. Fluid response model

The fluid response model has two parts. The first part models how blood volume responds to a fluid infusion based on control of blood and extravascular fluid-balance using a PI controller, similar to Refs. [10,11]. The second part models how SV responds to a change in blood volume with a linear relationship. The outcome is a model that calculates SV response to a fluid infusion input with 4 parameters, compared to 8 parameters for [11].

2.3.1. Blood volume control

The blood volume control model, similar to Refs. [10,11], is based on the physiological principle fluid volume distribution between intra-vascular and extra-vascular compartments aims to regulate the ratio of fluid change [19]. Thus, the target steady-state change in blood volume, $R_B(t)$, and extravascular volume, $R_E(t)$, in response to an input fluid flow, $F(t)$, is described in terms of the ratio α, yielding:

$$R_B(t) = \alpha \int_0^t F(\tau)d\tau \qquad R_E(t) = (1-\alpha)\int_0^t F(\tau)d\tau \tag{1}$$

Where $0 < \alpha < 1$, and a ratio of α:1-α fluid volume is absorbed into the blood and extra-vascular compartments respectively.

Flow to shift fluid from the blood to the extra-vascular compartment, $q(t)$, is a function of the error $e_B(t)$ between target $R_B(t)$ and actual blood volume change, $\Delta V_B(t)$, yielding:

$$e_B(t) = R_B(t) - \Delta V_B(t) \tag{2}$$

The relationship between $q(t)$ and $e_B(t)$ is modelled as a proportional-integral (PI) controller with proportional gain, K_P, and integral gain, K_I, defined:

$$q(t) = -K_p e_B(t) - K_i \int_0^t e_B(\tau)d\tau \tag{3}$$

Blood can only enter/leave the vascular compartment as $F(t)$ or $q(t)$, and can only enter/leave the extra-vascular compartment as $q(t)$. Thus conservation of blood volume means:

$$\Delta \dot{V}_B(t) = F(t) - q(t) \qquad \Delta \dot{V}_E(t) = q(t) \tag{4}$$

Combining Equations (1)–(4), the dynamics of $\Delta V_B(t)$ are governed by:

$$\Delta\ddot{V}_B(t) + K_p\Delta\dot{V}_B(t) + K_I\Delta V_B(t) = \dot{F}(t) + \alpha K_p F(t) + \alpha K_I \int_0^t F(\tau)d\tau \quad (5)$$

This equation has the closed-form solution, derived in full in Appendix A, given initial steady state conditions $\Delta V_B = 0, \Delta\dot{V}_B = 0$, defined:

$$\Delta V_B(t) = \frac{e^{-0.5t(K_p-\omega)}}{\omega}\int_0^t e^{0.5\tau(K_p-\omega)}g(\tau)d\tau - \frac{e^{-0.5t(K_p+\omega)}}{\omega}\int_0^t e^{0.5\tau(K_p+\omega)}g(\tau)d\tau \quad (6)$$

where $\omega = \sqrt{K_P^2 - 4K_I}$ and $g(t)$ is the right hand side of Equation (5). Note, ω is bounded to $0 < \omega < K_P$ so solutions are real-valued and overdamped.

Thus, from an input fluid infusion flow $F(t)$ and initial conditions of the system, in this case assumed steady state, changes in V_B can be predicted from Equation (6). ΔV_E can also be predicted from Equation (4), knowing predicted ΔV_B.

2.3.2. SV-blood volume relationship

SV is modelled as linearly related to V_B. Specifically, venous return, $Q_{VR}(t)$, can be expressed in terms of mean systemic filling pressure, P_{ms}, resistance to venous return, R, and P_{cv} [20,21]:

$$Q_{VR}(t) = \frac{P_{ms}(t) - P_{cv}(t)}{R} \quad (7)$$

where P_{ms} is the pressure arising from stressed blood volume, equal to the difference between V_B and unstressed blood volume, V_{BU}:

$$P_{ms} = \frac{V_B(t) - V_{BU}(t)}{C} \quad (8)$$

where C describes blood vessel compliance. Thus, combining these equations:

$$Q_{VR}(t) = \frac{V_B(t)}{RC} - \frac{V_{BU}(t)}{RC} - \frac{P_{cv}(t)}{R} \quad (9)$$

Beat-wise venous return volume SV_{VR} is on average equal to SV, to maintain equal inflow and outflow from the heart [22], yielding:

$$SV(t) = SV_{VR}(t) = \frac{Q_{VR}(t)}{f_{HR}} \quad (10)$$

where f_{HR} is heart rate.

Combing Equations (9) and (10), expressing blood volume in terms of an initial value, $V_{B,0}$, and its change, $V_B = V_{B,0} + \Delta V_B$, and assuming P_{cv}, V_{BU} and f_{HR} changes are small during the fluid infusion, then $SV(t)$ can be defined:

$$SV(t) = \frac{\Delta V_B(t)}{RCf_{HR}} + \frac{V_{B,0} - V_{BU}}{RCf_{HR}} - \frac{P_{cv}}{Rf_{HR}} \quad (11)$$

The constant term, $\frac{V_{B,0}-V_{BU}}{RCf_{HR}} - \frac{P_{cv}}{Rf_{HR}}$, is the SV component at initial state when $\Delta V_B = 0$, denoted SV_0. The term $\frac{1}{RCf_{HR}}$, lumped to be A, represents the proportion SV changes in response to V_B changes. Hence, the relationship between model-predicted SV_{fl} and V_B can be modelled as a linear relationship, defined:

$$SV_{fl}(t) = AV_B(t) + SV_0 \quad (12)$$

where, in this study SV_0 is identified for each fluid infusion separately by calibration using $\overline{SV_0}$, the average SV for first 50 beats of the infusion. Clinically, this calibration could be obtained via echocardiography, which, while adding workload, would have clinical value being used to guide decisions on delivering fluid therapy.

2.3.3. Parameter identification and model validation

The resulting fluid response model of Equations (6) and (12) has 4 parameters (K_P, ω, α, A). These parameters are identified from an input SV metric, $SV_{in}(t)$, by minimising the difference between $SV_{in}(t)$ and model-predicted $SV_{fl}(t)$ from Equation (12). SV_{mea} is used for SV_{in}, and is filtered with a 7-beat median filter, to reduce the impact of abnormal beats, such as extra-systoles, and an 18-beat moving average to reduce the impact of measurement noise and heart-lung interactions [23]. Clinically, SV_{in} could be obtained via echocardiography.

All four model parameters are identified simultaneously using the SciPy non-linear least squares optimisation function [24]. Parameters ω, α are bounded within their full ranges of $0 < \omega < K_P$ and $0 < \alpha < 1$, respectively. K_P is a positive parameter, constrained to $0 < K_P < 0.03$, where the upper limit of 0.03 s^{-1} anticipates fluid shift rates on a minute-hours timescale [19,25]. A is bounded to $0 < A < 0.3$, which is expected to encompass its full physiological range, given $A = 0.3$ represents a 3 ml SV increase in response to 10 ml increase in V_B.

Parameters are identified three different ways in this study:

1. Fitting parameters to the entire fluid infusion. This approach assess if the model accurately describes fluid-response profiles observed. Model-output SV from this method is labelled SV_{fl}^{Fit}, and these SV values assess model fit performance and accuracy compared to the measured dynamics.
2. Fitting parameters to the first 200 ml of the infusion only, and then using these parameters for predicting the remainder of the fluid infusion. This approach assesses if the model can predict fluid-response outcomes. SV from this method is labelled SV_{fl}^{200}, and these SV values quantify predictive accuracy.
3. Fitting parameters to the first 100 ml of the infusion only, and then using these parameters for predicting the remainder of the fluid infusion. This final analysis aims to assess if the model can predict fluid-response outcome from a small period at the beginning of the infusion. Fluid-response model outputs from this method are labelled SV_{fl}^{100}, and these values quantify predictive accuracy with a minimal calibration period.

The overall process for modelling SV response to a fluid infusion time-profile is shown in Fig. 2.

2.4. Analysis

Root mean squared error (RMSE) for SV from each parameter identification method (SV_{fl}^{Fit}, SV_{fl}^{200}, SV_{fl}^{100}) is calculated for each pig and fluid infusion. Mean RMSE is used compare the error for each method.

Model ability to predict SV trends is assessed by polar plot analysis [26] for each parameter identification method. A total of 200 beats are used from each fluid infusion, equally spaced across the infusion. For each beat, an X–Y pair of ΔSV percentage changes is calculated (X: ΔSV_{mea}, Y: ΔSV_{fl}). Polar angle (θ) is calculated as the angle of divergence of the ΔSV X–Y vector from the identity line Y = X. Radius is the percentage change of SV_{mea}. Trending ability is assessed using angular limits of agreement, defined as the larger value of the 2.5th & 97.5th percentile of θ, calculated with angles converted to a $[-90°, +90°]$ range. Only sufficiently large ΔSV are used in calculating limits of agreement, with small changes within a radius of $< 10\%$ ignored due to the impact of measurement noise. Acceptable angular limits of agreement are $\pm 30°$, based on those proposed for cardiac output monitoring [26], though noting this application is predicting SV response rather than monitoring it.

The ability of SV_{fl}^{200}, SV_{fl}^{100} to successfully predict both responsive and non-responsive infusions is assessed using receiver-operator characteristic (ROC) analysis [27]. An infusion is responsive if $\overline{SV}_{mea}(t_{end}) > 1.3 \times \overline{SV}_{mea}(t_{start})$, where t_{start} is the first 50 beats, and t_{end} is the final 50

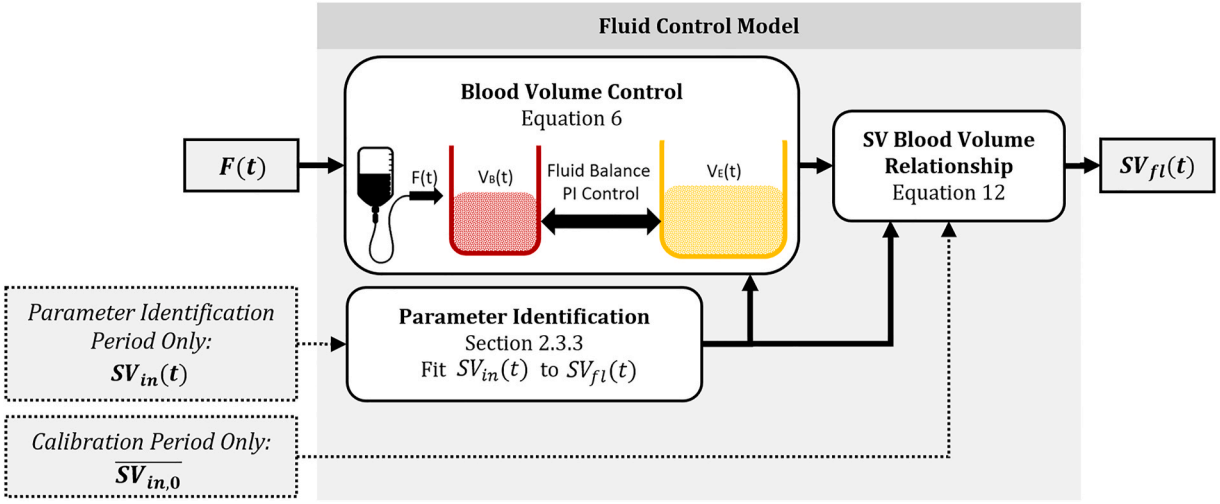

Fig. 2. Overview of fluid response model method, reading left to right. Model-based SV time-profile response, SV_{fl}, to input fluid infusion signal, $F(t)$, is predicted. The blood volume control model describes how $F(t)$ is balanced between V_B and V_E, modelled as PI control. The SV-V_B relationship converts V_B changes to an output prediction of SV_{fl}.

beats of the fluid infusion, and SV is averaged over these beats. The 30% increase threshold, compared 10–15% clinically [2,6], was chosen given SV is evaluated immediately as the infusion ends, and the large size of the fluid infusion for these pigs. Varying responsiveness threshold, c, where $SV_{fl}(t_{end}) > c \times SV_{fl}(t_{start})$, is used to produce a ROC curve of false positive rate (FPR) vs. true positive rate (TPR). The optimal cut-off threshold was chosen to maximise both sensitivity (TPR) and specificity ($1 - FPR$). Area under the curve (AUC) and balanced accuracy provide a measure of diagnostic accuracy of the model for identifying responsive and non-responsive infusions. High sensitivity and specificity in predicting non-responders would have the greatest clinical benefit in reducing iatrogenic harm in fluid therapy. SV_{fl}^{Fit} is calculated solely to verify model fit to observed SV dynamics, and thus is not included in ROC analysis.

For a reference fluid-responsiveness metric, a ROC curve was generated for stroke volume variation (SVV). SVV was chosen as it has the best clinical performance (AUC = 0.90) without requiring an additional test/manoeuvre in ventilated patients [28]. SVV is calculated using:

$$SVV = \frac{Max(SV(t_{start})) - Min(SV(t_{start}))}{\overline{SV(t_{start})}} \quad (13)$$

The statistical significance of ROC AUC differences for SV_{fl}^{200}, SV_{fl}^{100}, and SVV is compared using DeLong's test [29].

3. Results

Fig. 3 shows the time-series response of SV_{mea} and model-predicted SV_{fl} for each pig and fluid infusion. Fluid infusions led to an initial increase in SV, followed by a plateau and, in some cases, a decline in SV. All pigs had some response to the endotoxin infusion: reduced SV for Pigs 2, 4, and 5, and circulatory failure and death for Pigs 1, 3, and 6. The end-expiratory pauses induced a temporary SV spike, most notable for Pigs 1 and 3 (Fig. 3). Pig 5 had a short period of arrhythmia during fluid infusion 1, causing large SV variations at approximately 20 min through the infusion (Fig. 3).

The RMSE of each parameter identification method (SV_{fl}^{Fit}, SV_{fl}^{200}, SV_{fl}^{100}) for each pig and infusion, and overall, is given in Table 1. SV from optimal parameter identification, SV_{fl}^{fit}, had a good mean RMSE of 1.8 ml, and SV_{fl}^{200} had a reasonable mean RMSE of 3.2 ml. SV prediction from the first 100 ml of the infusion, SV_{fl}^{100}, was much poorer, with mean RMSE of 6.5 ml.

Polar plot analysis in Fig. 4 shows trending ability of model-predicted SV_{fl} compared to SV_{mea}, for each of the three parameter identification methods. The SV_{fl}^{fit} angular limit of agreement of 12°, indicates very good trending ability. Trending ability is reasonable for SV_{fl}^{200}, for which the angular limit of agreement of 28° meets the 30° acceptance criterion [26]. SV_{fl}^{100} angular limit of agreement of 69° is outside the acceptance criterion of 30°. Note, this large discrepancy is largely caused by ΔSVs just outside the exclusion radius, and most measurements are within smaller limits on the polar plot (Fig. 4).

ROC analysis to test the ability of SVV, SV_{fl}^{200}, and SV_{fl}^{100} to distinguish responsive and non-responsive infusions is shown in Fig. 5. Table 2 shows SVV and SV changes from SV_{mea}, SV_{fl}^{200}, and SV_{fl}^{100}, and whether each method correctly identified infusions as responsive/non-responsive. Using SV_{mea} there were 6 positive cases (responsive) and 6 negative cases (non-responsive). For SV_{fl}^{200} the optimal cut-off range was 1.6–1.7, for which there were 0 FP and 3 FN. For SV_{fl}^{100} the cut off range was 1.5–1.7 for which there were 1 FP and 2 FN. SV_{fl}^{200} and SV_{fl}^{100} had AUCs of 0.64 and 0.69, respectively, and both had a balanced accuracy of 0.75. For SVV the were 0 FP and 5 FN, with AUC of 0.39, and balanced accuracy of 0.58.

DeLong's test for difference in AUC of each ROC curve from Fig. 5 did not yield statistically significant differences ($p<0.05$) in any case. SV_{fl}^{200} vs. SVV had a p-value of 0.32, SV_{fl}^{100} vs. SVV had a p-value of 0.14, and SV_{fl}^{200} vs. SV_{fl}^{100} had a p-value of 0.81.

A summary of measured SV and arterial pressures for each pig and intervention is provided in appendix Table B1. Parameters from each parameter identification method are given in appendix Table B2.

4. Discussion

4.1. Response to fluid infusions

The overall response pattern of increasing SV until the end of the infusion followed by SV reduction (Fig. 3) matches clinical observations from Ref. [25]. The extent and rate of SV increase varied across pigs, providing a range of responses to test the model. In particular, the large/fatal responses to the endotoxin reflect the severe septic-shock induced, providing a robust test for the model that is similar to potential clinical use.

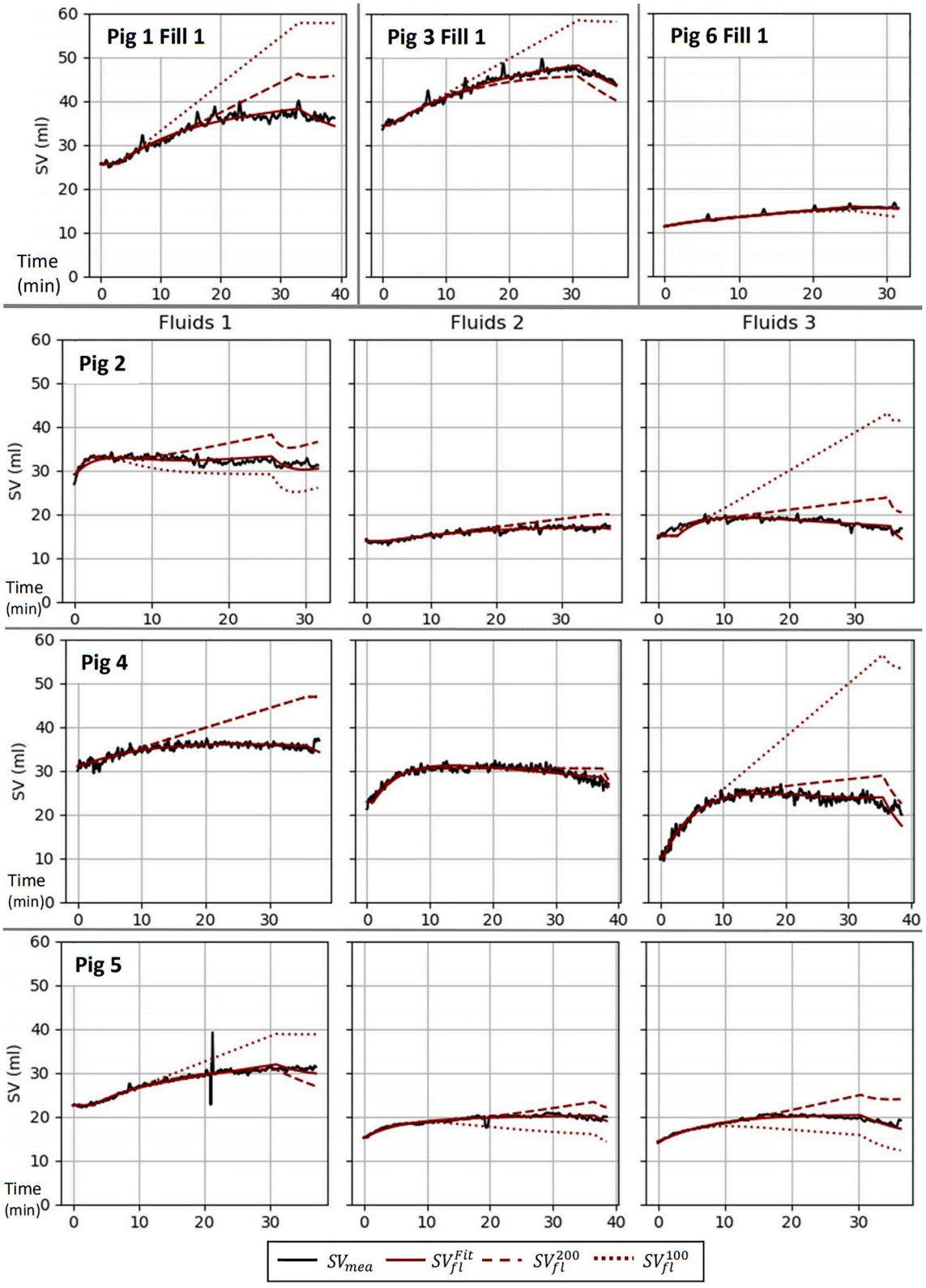

Fig. 3. SV time-profile for SV_{mea} and model-predicted SV (SV_{fl}^{Fit}, SV_{fl}^{200}, SV_{fl}^{100}) for each pig and fluid infusion.

4.2. Model performance

SV from optimal parameter identification, SV_{fl}^{fit} had very good fit and trending ability (Table 1, Fig. 4). This SV_{fl}^{fit} accuracy shows the fluid response model performs well and can fit the observed SV changes, and overall dynamics, indicating the model is suitable. SV prediction from the first 200 ml of the infusion, SV_{fl}^{200}, was good, whereas SV prediction from the first 100 ml of the infusion, SV_{fl}^{100}, was much poorer, with polar plot angular limit of agreement outside the acceptance criterion (Fig. 4).

When model-predicted SV_{fl}^{200} and SV_{fl}^{100} did perform poorly, they

Table 1
Root mean squared error (RMSE) for model-predicted SV from each parameter identification method: SV_{fl}^{Fit}, SV_{fl}^{200}, and SV_{fl}^{100}.

RMSE (ml)				
		SV_{fl}^{Fit}	SV_{fl}^{200}	SV_{fl}^{100}
Pig 1	Fluids 1	2.5	5.4	12.3
Pig 2	Fluids 1	2.2	3.9	3.8
	Fluids 2	1.3	1.9	1.9
	Fluids 3	1.3	3.6	14.0
Pig 3	Fluids 1	1.5	2.2	6.7
Pig 4	Fluids 1	2.1	6.2	6.2
	Fluids 2	2.1	2.2	2.2
	Fluids 3	3.5	4.5	18.5
Pig 5	Fluids 1	3.0	3.2	5.2
	Fluids 2	1.1	1.8	2.7
	Fluids 3	0.8	3.0	3.2
Pig 6	Fluids 1	0.4	0.4	0.8
Mean		**1.8**	**3.2**	**6.5**

tended to over-estimate SV increases, most substantially for Pigs 1 and 3 (Fig. 3). This over-estimation is a concern clinically, as wrongly identifying patients as fluid responsive could lead to fluid overload and poor patient outcome [1,30]. The overestimation of SV is potentially a systematic error which could be resolved by creating a weighting function to adjust predicted parameters.

These results show the fluid response model can potentially be used to predict SV trends in response to a fluid infusion. However, an adequate parameter identification period is required. In this pig trial, a 200 ml parameter identification period yielded good model performance, whereas 100 ml was insufficient. Longer parameter identification periods, such as 300 ml, would deliver even better model performance, but have less clinical value, as only the final 200 ml of the infusion is predicted. Clinically, model-predicted SV could be useful for guiding whether to continue a fluid infusion, or for closed loop fluid control [12,31].

ROC analysis to assess the ability of the model to classify responsive and non-responsive infusions showed similar performance of SV_{fl}^{100} and SV_{fl}^{200} (Fig. 5), likely because infusions with a large response overall responded well within the first 100 ml of the infusion. For SV_{fl}^{200} the optimal cut-off gave 0 FP and 3 FN, and for SV_{fl}^{100} the optimal cut-off gave 1 FP and 2 FN. Note, in a clinical setting, FPs are most problematic, given the potential harm of fluid overload. Differences in AUC are not statistically significant in any case, reflecting modest differences in AUC and that this ROC analysis is severely limited by low numbers (12). Further trials with a greater number of subjects and infusions is needed to better establish ability to classify responders/non-responders with this method.

4.3. Limitations

4.3.1. Experimental interventions

This study has a limited number of pigs and fluid infusions, in part due to the severity of the endotoxin infusion, causing the death of three pigs. In addition, a controlled pig trial differs from a clinical scenario, due to the controlled nature, and anatomical differences between pigs and humans. However, the pig trial enables initial proof of concept and demonstration of the method, to justify a further clinical investigation.

This experimental protocol could be improved upon for establishing parameter identification requirements. Future protocols could use different rate and duration of fluid infusions, and capture a period 'at rest' after each infusion. This would help to establish more clearly how to best administer a test bolus that would yield good parameter identification, and thus good SV prediction.

4.3.2. Model assumptions

The fluid response model is a simple model, lumping the spatially varying arterial properties and complex fluid balance mechanisms into just a four parameters. In doing so, it assumes various factors are constant, such heart rate and V_{BU}. To incorporate changes of these parameters, the model could be extended to describe how heart rate and vasoconstriction, thus V_{BU}, are regulated in response to the fluid infusion. Additionally, the model assumes initial steady state ($\Delta V_B = 0$, $\Delta \dot{V}_B = 0$), though an alternative known non-steady state could equally be used. For this proof-of-concept study, these modelling assumptions allow a simple clinically applicable model, which can predict response to a fluid infusion input time-profile.

The fluid response model in this study improves upon the more complex model from Ref. [11] for predicting fluid responsiveness. The

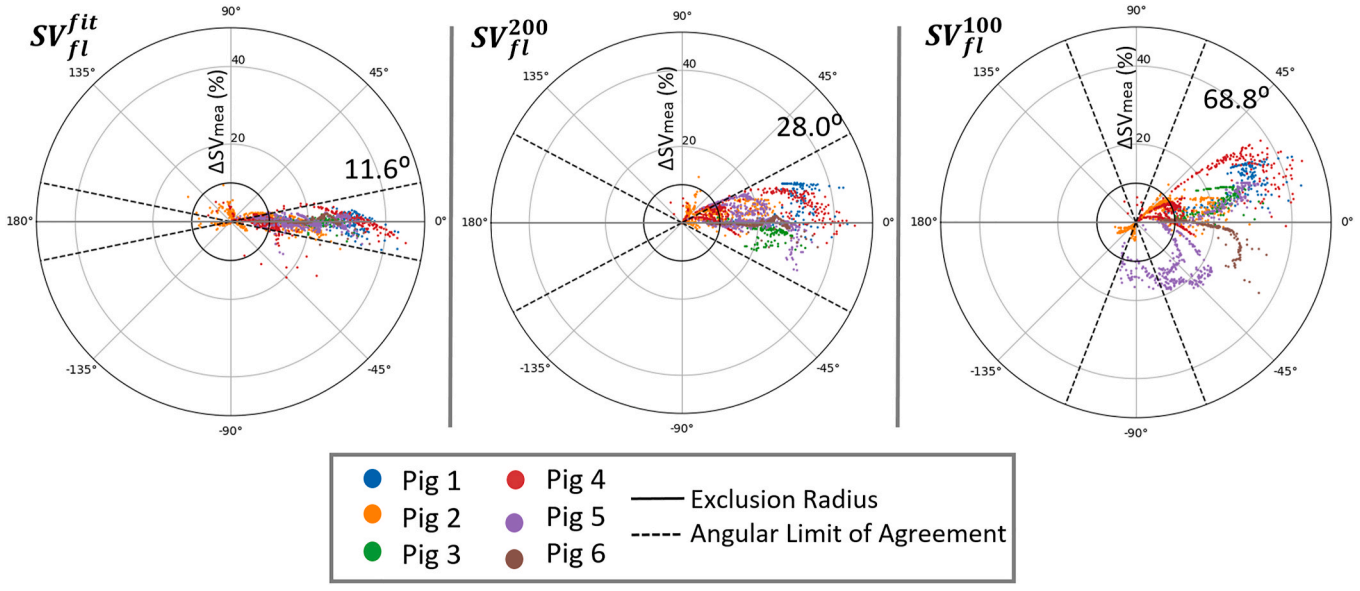

Fig. 4. Polar plot showing trending ability for model-predicted SV from each parameter identification method: SV_{fl}^{Fit}, SV_{fl}^{200}, and SV_{fl}^{100}. ΔSVs within a radius of 10% are excluded from angular limit of agreement calculation.

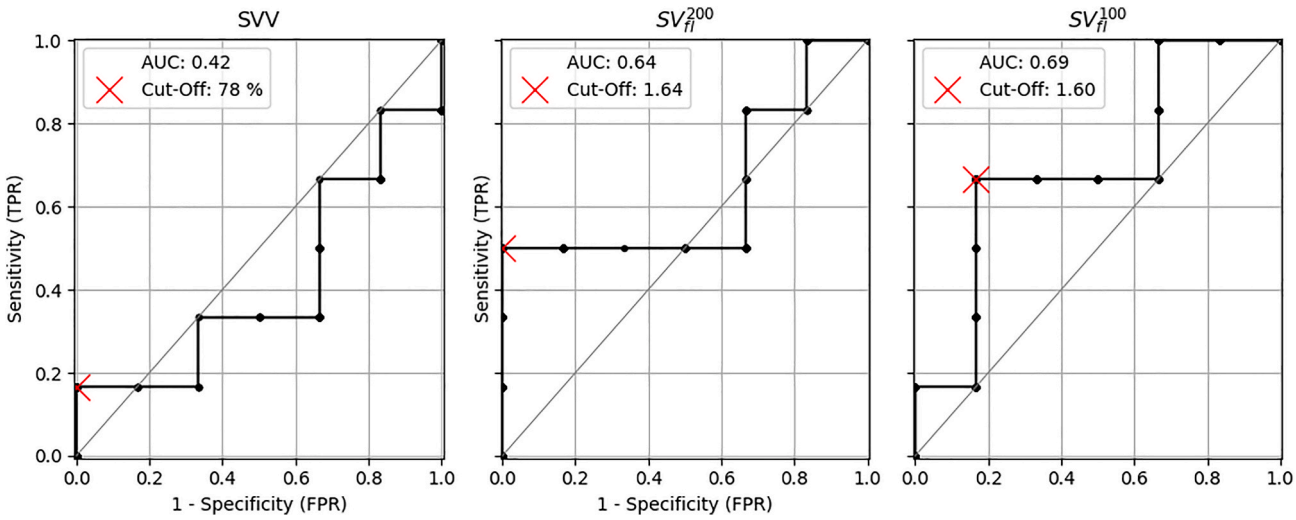

Fig. 5. ROC analysis for predicting responsive and non-responsive infusions from SVV, SV_{fl}^{200}, and SV_{fl}^{100}.

Table 2
SV proportional change (Δ, no units) at the end of each fluid infusion (t_{end}) relative to SV at the beginning of the infusion (t_{start}), from SV_{mea} and model-predicted SV_{fl}^{200}, and SV_{fl}^{100}. SVV (%) at the beginning of the infusion (t_{start}).

		SV_{mea}	SV_{fl}^{200}		SV_{fl}^{100}		SVV	
		Δ	Δ	T/F	Δ	T/F	%	T/F
Pig 1	Fluids 1	1.47	1.79	TP	2.24	TP	32	FN
Pig 2	Fluids 1	1.11	1.28	TN	0.98	TN	30	TN
	Fluids 2	1.19	1.44	TN	1.44	TN	34	TN
	Fluids 3	1.11	1.58	TN	2.85	FP	21	TN
Pig 3	Fluids 1	1.38	1.33	FN	1.69	TP	26	FN
Pig 4	Fluids 1	1.14	1.51	TN	1.51	TN	32	TN
	Fluids 2	1.22	1.33	TN	1.33	TN	33	TN
	Fluids 3	2.14	2.77	TP	5.40	TP	123	TP
Pig 5	Fluids 1	1.37	1.36	FN	1.71	TP	21	FN
	Fluids 2	1.29	1.50	TN	1.04	TN	15	TN
	Fluids 3	1.37	1.71	TP	1.09	FN	16	FN
Pig 6	Fluids 1	1.40	1.39	FN	1.31	FN	9	FN

blood volume control model from Ref. [11] can model response to blood loss via hemorrhage. However, for clinical prediction, identification of hemorrhage-associated parameters would require some blood volume reducing intervention, likely to worsen patient condition. Also, the relationship between SV and V_B in Ref. [11] requires an additional input of heart rate, meaning for predicting fluid responsiveness some way to predict heart rate changes is needed. Finally, the model from Ref. [11] avoids the need to assume P_{cv} is constant, through incorporating the empirical end-diastolic pressure-volume relationship. The outcome is a four-parameter Lambert W function relating SV to V_B and heart rate, which is not readily interpretable and likely unnecessarily complex. Overall, the model presented in this study resolves clinical applicability issues of the model from Ref. [11] for predicting fluid response time-profiles.

4.4. Translational considerations

Further clinical investigation is needed to establish the suitability of clinically feasible SV metrics as a model input, such as SV from echocardiography, and to find a suitable/optimal fluid bolus size and time-profile for identifying model parameters. Differences between the experimental pig trial and a clinical scenario mean that quantitative findings are not directly translatable. Thus, the established acceptable volume of 200 ml for the pig trial is not clinically pertinent, but this study provides a method to clinically identify an appropriate bolus size. In ICU, a typical fluid challenge is 250–500 ml [2,6], and recommended fluid resuscitation volume is 30 ml kg^{-1} [32]. Clinical validation should aim to establish if a volume less than or equal to a fluid-challenge can predict fluid resuscitation outcome.

This methodology considers fluid-response in terms of the time varying response to an infusion, acknowledging that there may be initial response to fluids that does not persist such as [25]. Clinically, it is important to consider how fluid responsiveness is defined, in terms of when the 10–15% SV increase should occur by, and how long it lasts for. This method has potential advantage over tests that simply predict binary classification of response/non-response as it predicts the time-profile of SV changes, which has clinical and monitoring benefits/utility.

To test fluid response in septic shock, it is important for consider the physiological causes of septic shock: loss of arterial tone, venous dilation, and micro-circulatory and myocardial dysfunction [30]. Preload-inducing tests, such as a passive leg raise, can establish cardiac/myocardial response to increased preload, identifying Frank-Starling contractility for the patient [33]. However a fluid input of some description is required to identify fluid-balance/fluid-exchange parameters, as for this method. These parameters are potentially useful in identifying how patients will dynamically respond to fluids.

5. Conclusions

This study presents a clinically-applicable, model-based method for predicting SV changes in response to a fluid infusion, validated for a pig trial. The model-predicted SV time-profiles match measured SV trends well, when the calibration/parameter identification period is sufficient. This trial is limited by small numbers, thus, it provides proof-of-method but further investigation is needed to establish clearly the calibration/parameter identification period requirements and clinical performance of this method. Potentially, the model-predicted SV time-profiles delivered could be used to guide fluid therapy decisions, or as part of a closed-loop fluid control system.

Declaration of competing interest

The authors declare that they have no conflicts of interest for the study titled “Predicting fluid-response, the heart of hemodynamic

management: a model-based solution" submitted to Computers in Biology and Medicine.

Acknowledgements

This work was supported with funding from the University of Canterbury Doctoral Scholarship, MedTech CoRE, Royal Society of New Zealand Engineering Technology-based Innovation in Medicine consortium grant, and EU FP7 International Research Staff Exchange Scheme. The funders had no role in study design, data collection and analysis, decision to publish or preparation of the manuscript.

A. Blood volume control model derivation

$\Delta V_B(t)$ dynamics are governed by Equation (5):

$$\Delta\ddot{V}_B(t) + K_p\Delta\dot{V}_B(t) + K_I\Delta V_B(t) = \dot{F}(t) + \alpha\frac{K_p}{F}(t) + \alpha\frac{K_I}{\int_0^t F(\tau)d\tau} \tag{A.1}$$

The solution ΔV_B is made up of a homogenous solution $\Delta V_{B,h}$ and particular solution $\Delta V_{B,p}$ [34].

$$\Delta V_B(t) = \Delta V_{B,h}(t) + \Delta V_{B,p}(t) \tag{A.2}$$

A.1. Homogenous solution

The homogenous solution $\Delta V_{B,h}$ solves the unforced system, given by:

$$\Delta\ddot{V}_B(t) + K_p\Delta\dot{V}_B(t) + K_I\Delta V_B(t) = 0 \tag{A.3}$$

Using the exponential substitution $\Delta V_B = Ae^{\lambda t}$ yields the following characteristic equation and roots:

$$\lambda^2 + K_p\lambda + K_I = 0 \qquad \lambda = \frac{-K_p \pm \sqrt{K_p^2 - 4K_I}}{2} \tag{A.4}$$

Substituting $\omega = \sqrt{K_p^2 - 4K_I}$ gives two ΔV_B, h components:

$$u_1 = e^{\frac{-t}{2}(K_p-\omega)} \qquad u_2 = e^{\frac{-t}{2}(K_p+\omega)} \tag{A.5}$$

Thus, the homogenous solution ΔV_B, h is:

$$\Delta V_{B,h}(t) = C_1e^{\frac{-t}{2}(K_p-\omega)} + C_2e^{\frac{-t}{2}(K_p+\omega)} \tag{A.6}$$

where C_1, C_2 are constants of integration, to be identified using initial conditions.

A.2. Particular solution

The particular solution ΔV_B, p solves the equation:

$$\Delta\ddot{V}_B(t) + K_p\Delta\dot{V}_B(t) + K_I\Delta V_B(t) = g(t) \tag{A.7}$$

where $g(t)$ is the right hand side of Equation (A.1). ΔV_B, p is found using the method of variation of parameters, which states that the solution will be [34]:

$$\Delta V_{B,p}(t) = -u_1(t)\int\frac{u_2(t)g(t)}{W(t)}dt + u_2(t)\int\frac{u_1(t)g(t)}{W(t)}dt \tag{A.8}$$

where W is the Wronskian [34], given by:

$$W(t) = u_1(t)\dot{u_2}(t) - u_2(t)\dot{u_1}(t) \tag{A.9}$$

Combing Equations (A.9) and (A.5) then W can be expressed as:

$$W(t) = \frac{-(K_p+\omega)}{2}e^{\frac{-t}{2}(K_p-\omega)}e^{\frac{-t}{2}(K_p+\omega)} - \frac{-(K_p-\omega)}{2}e^{\frac{-t}{2}(K_p+\omega)}e^{\frac{-t}{2}(K_p-\omega)} \tag{A.10}$$

Simplifying to:

$$W(t) = -\omega e^{-K_pt} \tag{A.11}$$

Thus, combining Equations (A.8), (A.11), and (A.5) yields an expression for $\Delta V_{B,p}$:

$$\Delta V_{B,p}(t) = -e^{\frac{-t}{2}(K_p-\omega)}\int\frac{e^{\frac{-t}{2}(K_p+\omega)}g(t)}{-\omega e^{-K_pt}}dt + e^{\frac{-t}{2}(K_p+\omega)}\int\frac{e^{\frac{-t}{2}(K_p-\omega)}g(t)}{-\omega e^{-K_pt}}dt \tag{A.12}$$

Simplifying to:

$$\Delta V_{B,p}(t) = \frac{e^{\frac{-t}{2}(K_p-\omega)}}{\omega}\int e^{\frac{t}{2}(K_p-\omega)}g(t)dt + \frac{-e^{\frac{-t}{2}(K_p+\omega)}}{\omega}\int e^{\frac{t}{2}(K_p+\omega)}g(t)dt \tag{A.13}$$

A.3. Initial conditions

The overall solution ΔV_B is from combining Equations (A.2), (A.6) and (A.13):

$$\Delta V_B(t) = C_1 e^{\frac{-t}{2}(K_p-\omega)} + C_2 e^{\frac{-t}{2}(K_p+\omega)} + \frac{e^{\frac{-t}{2}(K_p-\omega)}}{\omega}\int e^{\frac{t}{2}(K_p-\omega)}g(t)dt + \frac{-e^{\frac{-t}{2}(K_p+\omega)}}{\omega}\int e^{\frac{t}{2}(K_p+\omega)}g(t)dt \tag{A.14}$$

The derivative of Equation (A.14) is:

$$\begin{aligned}\Delta \dot{V}_B(t) = &-C_1\frac{K_p-\omega}{2}e^{\frac{-t}{2}(K_p-\omega)} - C_2\frac{K_p+\omega}{2}e^{\frac{-t}{2}(K_p+\omega)} - \frac{K_p-\omega}{2\omega}e^{\frac{-t}{2}(K_p-\omega)}\int e^{\frac{t}{2}(K_p-\omega)}g(t)dt \\ &+\frac{K_p+\omega}{2\omega}e^{\frac{-t}{2}(K_p+\omega)}\int e^{\frac{t}{2}(K_p+\omega)}g(t)dt\end{aligned} \tag{A.15}$$

Evaluating initial zero condition $\Delta V_B(0) = 0$ for Equation (A.14) gives:

$$\Delta V_B(0) = C_1 e^0 t + C_2 e^0 + \frac{e^0}{\omega}\int_{\tau=0}^{\tau=0} e^{\frac{\tau}{2}(K_p-\omega)}g(\tau)d\tau + \frac{-e^0}{\omega}\int_{\tau=0}^{\tau=0} e^{\frac{\tau}{2}(K_p+\omega)}g(\tau)d\tau = 0 \tag{A.16}$$

Simplifying to:

$$C_1 + C_2 = 0 \tag{A.17}$$

Evaluating initial steady-state condition $\Delta \dot{V}_B(0) = 0$ for Equation A.15 yields:

$$\begin{aligned}\Delta \dot{V}_B(0) = &-C_1\frac{K_p-\omega}{2}e^0 - C_2\frac{K_p+\omega}{2}e^0 - \frac{K_p-\omega}{2\omega}e^0\int_{\tau=0}^{\tau=0} e^{\frac{\tau}{2}(K_p-\omega)}g(\tau)d\tau \\ &+\frac{K_p+\omega}{2\omega}e^0\int_{\tau=0}^{\tau=0} e^{\frac{\tau}{2}(K_p+\omega)}g(\tau)d\tau = 0\end{aligned} \tag{A.18}$$

Simplifying to:

$$C_1\frac{-(K_p-\omega)}{2} + C_2\frac{-(K_p+\omega)}{2} = 0 \tag{A.19}$$

$$K_p(C_1+C_2) + \omega(C_2-C_1) = 0 \tag{A.20}$$

Combining Equations (A.17) and (A.20) yields:

$$C_1 = C_2 = 0 \tag{A.21}$$

Using these values of C_1, C_2 in Equation A.14 yields the solution, as in Equation (6):

$$\Delta V_B(t) = \frac{e^{-0.5t(K_p-\omega)}}{\omega}\int_0^t e^{0.5\tau(K_p-\omega)}g(\tau)d\tau - \frac{e^{-0.5t(K_p+\omega)}}{\omega}\int_0^t e^{0.5\tau(K_p+\omega)}g(\tau)d\tau \tag{A.22}$$

B. Additional results

Table B1
Summary of P_{arch} and SV_{mea} during each fluid infusion for each pig. Values are presented as mean [2.5th,97.5th percentile]. $\overline{P}$ refers to beat-wise pressure, and *PP* refers to pulse pressure. N is the number of heart beats.

		N	$\overline{P}_{arch}$	P_{arch} *PP*	SV_{mea}
			mmHg		*ml*
Pig 1	Fluids 1	2270	63 [55, 65]	30 [24,31]	34 [24,41]
Pig 2	Fluids 1	1984	58 [56, 60]	27 [25,29]	32 [29, 35]
	Fluids 2	2513	54 [51, 56]	31 [25,33]	16 [13,18]
	Fluids 3	2413	50 [47, 52]	32 [28,34]	18 [15,20]
Pig 3	Fluids 1	2676	54 [45, 56]	28 [23,30]	44 [34, 49]
Pig 4	Fluids 1	3312	84 [77, 87]	36 [31, 38]	35 [29, 39]
	Fluids 2	3156	64 [50, 67]	32 [24,34]	30 [23,34]
	Fluids 3	3144	46 [33, 49]	31 [19,32]	23 [9,29]
Pig 5	Fluids 1	2510	46 [43, 48]	23 [21,24]	29 [22,33]
	Fluids 2	2306	36 [33, 40]	19 [15,21]	19 [15,21]
	Fluids 3	2150	43 [36, 44]	24 [17,25]	19 [15,21]
Pig 6	Fluids 1	2291	50 [48, 51]	22 [19,24]	14 [11,16]

Table B2
Fluid-balance model parameters identified by each parameter identification method: fitting to the entire fluid infusion (Fit), fitting to the first 200 ml of the 500 ml infusion (200), and fitting to the first 100 ml of the infusion (100).

		$100K_P$ $(\frac{1}{s})$			100ω $(\frac{1}{s})$			α (No units)			$10A$ (No units)		
		Fit	200	100	Fit	200	100	Fit	200	100	Fit	200	100
Pig 1	Fluids 1	0.19	1.35	0.00	0.00	0.00	0.92	0.26	0.42	1.00	0.63	0.97	0.64
Pig 2	Fluids 1	0.79	1.40	1.08	0.00	0.01	0.00	0.08	0.09	0.00	1.06	1.94	1.83
	Fluids 2	0.09	0.60	0.00	0.00	0.19	0.00	0.00	1.00	0.71	0.15	0.12	0.12
	Fluids 3	0.48	2.33	2.90	0.77	1.00	0.00	0.00	0.04	0.19	1.06	3.00	3.00
Pig 3	Fluids 1	0.10	0.10	0.56	0.00	0.00	0.41	0.16	0.00	1.00	0.55	0.56	0.48
Pig 4	Fluids 1	0.13	0.66	0.66	0.00	0.21	0.21	0.00	1.00	1.00	0.51	0.32	0.32
	Fluids 2	0.37	0.66	0.66	0.81	1.00	1.00	0.00	0.00	0.00	1.60	2.26	2.26
	Fluids 3	0.30	0.39	1.25	0.00	0.91	1.00	0.10	0.08	0.31	1.98	2.18	2.72
Pig 5	Fluids 1	0.32	0.11	3.00	0.00	0.00	1.00	0.37	0.00	0.74	0.45	0.42	0.43
	Fluids 2	0.31	0.69	0.36	1.00	0.00	0.00	0.03	0.19	0.00	0.58	0.85	0.73
	Fluids 3	0.20	0.73	0.33	0.00	0.00	0.00	0.13	0.37	0.00	0.42	0.58	0.54
Pig 6	Fluids 1	0.48	0.57	0.11	0.00	0.00	0.00	0.54	0.46	0.00	0.16	0.19	0.16
Mean		0.31	0.80	0.91	0.08	0.30	0.44	0.14	0.30	0.41	0.76	1.12	1.10
Range		0.70	2.23	3.00	0.37	2.33	3.00	0.54	1.00	1.00	1.83	2.88	2.88

References

[1] A. Carsetti, M. Cecconi, A. Rhodes, Fluid bolus therapy, Curr. Opin. Crit. Care 21 (2015) 388–394.
[2] F. Michard, J.-L. Teboul, Predicting fluid responsiveness in icu patients, Chest 121 (2002) 2000–2008.
[3] J.-L. Vincent, Y. Sakr, C.L. Sprung, V.M. Ranieri, K. Reinhart, H. Gerlach, R. Moreno, J. Carlet, J.-R.L. Gall, D. Payen, et al., Sepsis in european intensive care units: results of the soap study, Crit. Care Med. 34 (2006) 344–353.
[4] R. Gaudet, R. Kalman, Comparison of Two Fluid-Management Strategies in Acute Lung Injury, 50 Studies Every Intensivist Should Know, 2018, pp. 141–146.
[5] J.H. Boyd, J. Forbes, T.-A. Nakada, K.R. Walley, J.A. Russell, Fluid resuscitation in septic shock: a positive fluid balance and elevated central venous pressure are associated with increased mortality, Crit. Care Med. 39 (2011) 259–265.
[6] X. Monnet, P.E. Marik, J.-L. Teboul, Prediction of fluid responsiveness: an update, Ann. Intensive Care 6 (2016).
[7] B.A. Jalil, R. Cavallazzi, Predicting fluid responsiveness: a review of literature and a guide for the clinician, Am. J. Emerg. Med. 36 (2018) 2093–2102.
[8] M. Cecconi, D. De Backer, M. Antonelli, R. Beale, J. Bakker, C. Hofer, R. Jaeschke, A. Mebazaa, M.R. Pinsky, J. Louis, T. Jean, L. Vincent, A. Rhodes, M. Cecconi, Á. A. Rhodes, D. De Backer, J.L. Vincent, M. Antonelli, R. Beale, J. Bakker, C. Hofer, R. Jaeschke, P. Diderot, P. Sorbonne, P. Cité, L. Aphp, M.R. Pinsky, J.L. Teboul, Consensus on circulatory shock and hemodynamic monitoring. Task force of the European Society of Intensive Care Medicine, Intensive Care Med. 40 (2014) 1795–1815.
[9] P. Bentzer, D.E. Griesdale, J. Boyd, K. Maclean, D. Sirounis, N.T. Ayas, Will this hemodynamically unstable patient respond to a bolus of intravenous fluids? Jama 316 (2016) 1298.
[10] R. Bighamian, A.T. Reisner, J.-O. Hahn, A lumped-parameter subject-specific model of blood volume response to fluid infusion, Front. Physiol. 7 (2016).
[11] R. Bighamian, B. Parvinian, C.G. Scully, G. Kramer, J.-O. Hahn, Control-oriented physiological modeling of hemodynamic responses to blood volume perturbation, Control Eng. Pract. 73 (2018) 149–160.
[12] T. Desaive, O. Horikawa, J.P. Ortiz, J.G. Chase, Model-based management of cardiovascular failure: where medicine and control systems converge, Annu. Rev. Control 48 (2019) 383–391.
[13] J.G. Chase, G.M. Shaw, J.-C. Preiser, J.L. Knopp, T. Desaive, Risk-based care: lets think outside the box, Front. Med. 8 (2021).
[14] F. Gavelli, J.-L. Teboul, X. Monnet, The end-expiratory occlusion test: please, let me hold your breath, Crit. Care 23 (2019).
[15] M. Merx, C. Weber, Sepsis and the heart, Circulation 116 (2007) 793–802.
[16] J. Balmer, C. Pretty, S. Davidson, T. Desaive, S. Kamoi, A. Pironet, P. Morimont, N. Janssen, B. Lambermont, G.M. Shaw, J.G. Chase, Pre-ejection period, the reason why the electrocardiogram Q-wave is an unreliable indicator of pulse wave initialization, Physiol. Meas. 39 (2018), 095005.
[17] X.X. Yang, L.A. Critchley, D.K. Rowlands, Z. Fang, L. Huang, Systematic error of cardiac output measured by bolus thermodilution with a pulmonary artery catheter compared with that measured by an aortic flow probe in a pig model, J. Cardiothorac. Vasc. Anesth. 27 (2013) 1133–1139.
[18] S. Kutty, A.T. Kottam, A. Padiyath, K.R. Bidasee, L. Li, S. Gao, J. Wu, J. Lof, D. A. Danford, T. Kuehne, et al., Validation of admittance computed left ventricular volumes against real-time three-dimensional echocardiography in the porcine heart, Exp. Physiol. 98 (2013) 1092–1101.
[19] J.E. Hall, A.C. Guyton, Guyton and Hall Textbook of Medical Physiology, Elsevier, 2016.
[20] W.G. Parkin, Volume state control - a new approach, Crit. Care Resuscitation 1 (1999) 311–321.
[21] A.C. Guyton, A.W. Lindsey, B. Abernathy, T. Richardson, Venous return at various right atrial pressures and the normal venous return curve, Am. J. Physiol. Legacy Content 189 (1957) 609–615.
[22] F. Starling, The linacre lecture on the law of the heart given at cambridge, 1915, Nature 101 (1918) 43.
[23] M.R. Pinsky, D. Payen, Functional hemodynamic monitoring, Crit. Care 9 (2005) 566.
[24] P. Virtanen, R. Gommers, T.E. Oliphant, M. Haberland, T. Reddy, D. Cournapeau, E. Burovski, P. Peterson, W. Weckesser, J. Bright, S.J. van der Walt, M. Brett, J. Wilson, K.J. Millman, N. Mayorov, A.R.J. Nelson, E. Jones, R. Kern, E. Larson, C. J. Carey, İ. Polat, Y. Feng, E.W. Moore, J. VanderPlas, D. Laxalde, J. Perktold, R. Cimrman, I. Henriksen, E.A. Quintero, C.R. Harris, A.M. Archibald, A.H. Ribeiro, F. Pedregosa, P. van Mulbregt, SciPy 1.0 contributors, SciPy 1.0: fundamental algorithms for scientific computing in Python, Nat. Methods 17 (2020) 261–272.
[25] T.S.O. Nunes, R.T. Ladeira, A.T. Bafi, L.C.P.D. Azevedo, F.R. Machado, F.G. R. Freitas, Duration of hemodynamic effects of crystalloids in patients with circulatory shock after initial resuscitation, Ann. Intensive Care 4 (2014).
[26] L.A. Critchley, X.X. Yang, A. Lee, Assessment of trending ability of cardiac output monitors by polar plot methodology, J. Cardiothorac. Vasc. Anesth. 25 (2011) 536–546.
[27] K.H. Zou, A.J. O'Malley, L. Mauri, Receiver-operating characteristic analysis for evaluating diagnostic tests and predictive models, Circulation 115 (2007) 654–657.
[28] J.I.A. Sánchez, J.D.C. Ruiz, J.J.D. Fernández, W.F.A. Zuñiga, G.A. Ospina-Tascón, L.E.C. Martínez, Predictors of fluid responsiveness in critically ill patients mechanically ventilated at low tidal volumes: systematic review and meta-analysis, Ann. Intensive Care 11 (2021).
[29] E.R. DeLong, D.M. DeLong, D.L. Clarke-Pearson, Comparing the areas under two or more correlated receiver operating characteristic curves: a nonparametric approach, Biometrics 44 (1988) 837.
[30] P. Marik, R. Bellomo, A rational approach to fluid therapy in sepsis, Br. J. Anaesth. 116 (2016) 339–349.
[31] R. Bighamian, C.-S. Kim, A.T. Reisner, J.-O. Hahn, Closed-loop fluid resuscitation control via blood volume estimation, J. Dyn. Syst. Meas. Control 138 (2016).
[32] A. Rhodes, L.E. Evans, W. Alhazzani, M.M. Levy, M. Antonelli, R. Ferrer, A. Kumar, J.E. Sevransky, C.L. Sprung, M.E. Nunnally, B. Rochwerg, G.D. Rubenfeld, D. C. Angus, D. Annane, R.J. Beale, G.J. Bellinghan, G.R. Bernard, J.-D. Chiche, C. Coopersmith, D.P.D. Backer, C.J. French, S. Fujishima, H. Gerlach, J.L. Hidalgo, S.M. Hollenberg, A.E. Jones, D.R. Karnad, R.M. Kleinpell, Y. Koh, T.C. Lisboa, F. R. Machado, J.J. Marini, J.C. Marshall, J.E. Mazuski, L.A. McIntyre, A.S. McLean, S. Mehta, R.P. Moreno, J. Myburgh, P. Navalesi, O. Nishida, T.M. Osborn, A. Perner, C.M. Plunkett, M. Ranieri, C.A. Schorr, M.A. Seckel, C.W. Seymour, L. Shieh, K.A. Shukri, S.Q. Simpson, M. Singer, B.T. Thompson, S.R. Townsend, T.

V. der Poll, J.-L. Vincent, W.J. Wiersinga, J.L. Zimmerman, R.P. Dellinger, Surviving sepsis campaign, Crit. Care Med. 45 (2017) 486–552.
[33] R. Smith, J.G. Chase, C.G. Pretty, S. Davidson, G.M. Shaw, T. Desaive, Preload & frank-starling curves, from textbook to bedside: clinically applicable non-additionally invasive model-based estimation in pigs, Comput. Biol. Med. 135 (2021) 104627.
[34] G. Teschl, Ordinary Differential Equations and Dynamical Systems, American Mathematical Society, 2020.